should be the same as for Au–Cl in $AuCl_2^-$ (note that Au has a closed (d^{10}) electron configuration, and any eventual d to p back-bonding can be neglected). Structures different from the centrosymmetric one for ICl_2^- are expected to be as unlikely as they are for $AuCl_2^-$. However, short-lived intermediates with chlorine as central atom might exist among the heteronuclear trihalide anions. That follows directly from the similarities in orbital symmetry and electron population discussed earlier.

Acknowledgment. I am very grateful to Dr. A. Sandell for the help with the computer calculations, to Dr. L. I. Elding for valuable suggestions and positive criticism of the manuscript, and to B. Jönsson and E. Bredenfeldt for experimental assistance. Thanks are also due to O. Hansson for skillful technical assistance. The Swedish Natural Science Research Council (NFR) is thanked for financial support.

Appendix

The formation of ICl_4^- according to eq 43 is known from preparative polyhalogen chemistry.[2,38] The reaction may possibly

$$I^- + 2Cl_2 \rightarrow ICl_4^- \quad (43)$$

occur in the solutions studied here, at least when C_{Cl_2} is high (cf. Table II, series a) and $C_I < {}^1/_2C_{Cl_2}$, i.e. when $v < v_{EP}(0)$ (cf. Figure 3a). Besides eq 43, eq 2 is valid and we can write (44). The

$$Cl_2 + ICl_2^- \rightleftarrows ICl_4^- \quad (44)$$

stoichiometry is given by (45) and (46). If it is assumed that

$$C_{Cl_2} = [Cl_2] + [Cl_3^-] + [ICl_2^-] + 2[ICl_4^-] \quad (45)$$

$$C_I = [ICl_2^-] + [ICl_4^-] \quad (46)$$

the equilibrium according to eq 44 is displaced to the right when $v < v_{EP}(0)$, then $[ICl_2^-] \ll [ICl_4^-]$ and the relevant concentrations can simply be calculated from eq 47 and 48. When all added

$$[ICl_4^-] = C_I \quad (47)$$

$$[Cl_2] + [Cl_3^-] = C_{Cl_2} - 2C_I \quad (48)$$

I^- has been converted to ICl_4^-, $v = v_{EP}(0)$. As discussed earlier, $v = v_{EP}(1)$, when all I^- has been converted to ICl_2^-. It follows that (49) holds true, and the measurements displayed in Figure

$$v_{EP}(0) = {}^1/_2v_{EP}(1) \quad (49)$$

3a show that this condition is fullfilled. The curve is based on series a, and the values in the appropriate volume region are given in Table V. It has been assumed that the emf-determining process is given by eq 25, with $[Cl_2]$ calculated from eq 48 and eq 1. The values for $E_{25}°$ (1127.1 mV) and slope (24.1 mV) are sufficiently close to those calculated earlier (1132.0 and 27.2 mV, respectively) to validate the assumptions made.

In the range $v_{EP}(0) < v < v_{EP}(1)$ it is assumed that ICl_4^- reacts with added I^- to give ICl_2^- and that the half-cell reaction is

$$ICl_4^- + 2e^- \rightarrow ICl_2^- + 2Cl^- \quad (50)$$

This can be combined with eq 23 to give the total cell reaction. The emf, E_{51}, is given by

$$E_{51} = E_{51}° - ((RT \ln 10)/2F) \log ([ICl_2^-]/[ICl_4^-]) \quad (51)$$

The concentrations can be calculated from eq 45 and 46 with $[Cl_2] = [Cl_3^-] = 0$. The result is shown in Table V. Combining the two half-cell reactions (50) and (24) gives eq 44. The equilibrium constant K_{44} can be calculated from eq 52. Inserting the earier determined value of $E_{25}°$ (1132.0 mV) or $E_{25}°$ from Table V results in $K_{44} = 4.3\ (5) \times 10^3\ M^{-1}$. From this value we can

$$((RT \ln 10)/2F) \log K_{44} = E_{25}° - E_{51}° \quad (52)$$

conclude that the concentration of ICl_2^- never exceeds 6×10^{-4} M when $v < v_{EP}(0)$. However, it means that eq 47 and 48 are only approximately valide. If a correction for ICl_2^- is applied to the calculated values of $[Cl_2]$ in Table V, $E_{25}°$ increases to 1129.1 mV and the slope to 25.3 mV. This is closer to the corresponding quantities in Table II than the original ones in Table V.

Registry No. Cl_3^-, 18434-33-8; I_3^-, 14900-04-0; ICl_2^-, 14522-79-3; I_2Cl^-, 17705-05-4.

Supplementary Material Available: Tables of spectrophotometric data giving total concentrations of halogen molecules and halide ions and absorptivities at several wavelengths and potentiometric data giving volumes of added reagent (I^-), emf, and calculated concentrations of the relevant species (cf. the text preceding eq 26 and 40) (15 pages). Ordering information is given on any current masthead page.

(38) Popov, A. I.; Buckles, R. E. *Inorg. Synth.* **1957**, *5*, 176.

Contribution from the Departments of Chemistry, Brown University, Providence, Rhode Island 02912, and Queen Mary College, London E1 4NS, England

Effect on Redox Potentials of Hydrogen Bonding from Coordinated Imidazole in Metalloporphyrin Complexes

P. O'BRIEN*[1] and D. A. SWEIGART*[2]

Received October 26, 1984

The Fe(III)/Fe(II) reduction potentials for [Fe(porphyrin)(imidazole)$_2$]X (porphyrin = TPP, PPIXDME; imidazole = HIm, *N*-MeIm; X = Cl^-, SbF_6^-) have been measured by cyclic voltammetry in a variety of solvents. The addition of excess imidazole or 1,10-phenanthroline (phen) to Fe(porphyrin)$(HIm)_2^+$ cause a cathodic shift of ca. 60 mV in the reduction potential, and this shift is assigned to a hydrogen-bonding interaction between the coordinated imidazole N–H and free imidazole or phen. In support of this, excess phen was found to have no effect on $E_{1/2}$ for Fe(porphyrin)$(N\text{-MeIm})_2^+$. The $E_{1/2}$ values measured relative to the ferrocene/ferrocenium couple correlate well with the solvent dielectric constant and donor number, although a simple interpretation of this correlation is not possible. Experiments were done with tetra-*n*-butylammonium perchlorate (TBAP) and tetra-*n*-butylammonium tetraphenylborate ((TBA)BPh_4) as the supporting electrolyte, and these show that ClO_4^- from TBAP also can hydrogen bond to coordinated imidazole. A discussion is given of these hydrogen-bonding interactions, as well as ion-pairing effects. The studies show that the redox potential changes due to hydrogen bonding from coordinated imidazole in Fe(porphyrin)$(HIm)_2^+$ is of sufficient magnitude to be considered seriously as a mechanism of redox potential regulation in heme proteins. The $E_{1/2}$ for Ru(TPP)(CO)(HIm) oxidation was found not to be influenced by phen, and it is concluded that hydrogen-bonding effects are only important when the redox change is metal centered, as with Fe(III)/Fe(II), instead of porphyrin ring centered as with Ru(TPP)(CO)(HIm) oxidation, which gives a Ru(II) cation radical.

Introduction

Variations in reactivity of the iron center in heme proteins are determined primarily by the axial ligands, the most common of which is imidazole (HIm) from a "proximal" histidine residue. Perhaps the best known example of reactivity modulation is the trigger mechanism for hemoglobin cooperativity, in which movement of the iron atom toward the porphyrin plane is restrained by virtue of the imidazole ring orientation.[3] This restraint

0020-1669/85/1324-1405$01.50/0

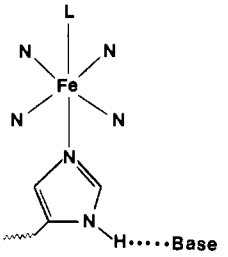

Figure 1. Proximal type hydrogen bonding from a coordinated imidazole N–H to an external base.

is relaxed when the protein conformation changes from the T state to the R state.

Another way the proximal histidine can influence heme reactivity is via hydrogen bonding or deprotonation of the imidazole N–H proton (Figure 1). As the level of hydrogen-bonding increases, the donor ability of the imidazole imine nitrogen also increases, resulting in a stronger Fe–N bond and more electron density on the iron. Of course, the limit of strong hydrogen bonding corresponds to deprotonation, and it is known that coordination to the metal increases the acidity of the imidazole N–H proton by ca. 4 pK_a units in metmyoglobin[4,5] and inorganic complexes such as $(H_3N)_5Co(HIm)^{3+}$ and $(NC)_5Fe(HIm)^{2-}$.[6,7]

Resonance Raman and NMR studies[8-11] of horseradish and turnip peroxidases suggest that the proximal histidine is strongly bonded or even deprotonated. X-ray structural and NMR data indicate similar results for cytochrome *c* peroxidase.[12,13] EPR spectra show that the level of proximal histidine hydrogen bonding varies in a series of cytochrome *c* enzymes.[14] Strong proximal hydrogen bonding should favor higher oxidation states and may account for the ease with which peroxidases are oxidized compared to the oxygen carriers hemoglobin and myoglobin, in which the hydrogen bonding is weaker.[8,11,13,15] Variations in the proximal hydrogen-bond strength has been suggested to influence or be coupled to the thermodynamics and kinetics of ligand binding, protein conformational changes, the cooperative of hemoglobin, the O_2/CO affinity ratio of hemoglobin, and redox potential modulation in heme proteins.[15-24]

Hydrogen-bonding effects have been observed with simple metalloporphyrin model systems. The formation constants for [Fe(porphyrin)$(HIm)_2$]Cl are greatly enhanced compared to the corresponding *N*-methylimidazole complexes because the coordinated imidazole N–H hydrogen bonds to the chloride anion or free imidazole in solution.[25] The nonnucleophilic base, 1,10-phenanthroline was shown to associate with the N–H groups in bis(imidazole)metalloporphyrins, thereby affecting stability constants and NMR spectra.[26] Several groups have prepared and characterized Fe(porphyrin)$(Im)_2^-$ complexes, which contain deprotonated imidazole ligands.[27-29] Hydrogen bonding is reported to affect the resonance Raman iron–imidazole vibration in Fe(II) porphyrins[19] but is claimed[30] to have little influence on CO binding; the effect on O_2 binding to model systems is unknown. However, CO affinity is substantially reduced when the coordinated imidazole is deprotonated to give anionic iron(II) porphyrin complexes.[15,23] Furthermore, deprotonation greatly reduces the CO association rate constant while hydrogen bonding of the N–H link to 1,10-phenanthroline leads to a modest decrease in the rate constant.[20]

Fe(III)/Fe(II) reduction potentials for oxygen-carrying heme proteins can be shifted 100 mV or more as a result of the specific interaction of the heme and apoprotein.[8,31] This is even more clearly shown by a comparison of cytochrome *c* peroxidase and myoglobin. The axial ligand environments of the protoheme are the same[12] (histidine and water ligands in the ferric protein) yet the reduction potentials are −194 and +50 mV, respectively.[13,32,33] It has been suggested that hydrogen bonding by the proximal histidine in cytochrome *c* peroxidase is stronger and more easily varied, thereby providing a mechanism for redox potential regulation during the catalytic cycle.[13]

Attempts to understand the role of hydrogen bonding in redox potential modulation in proteins have recently been made by investigating the redox chemistry of simple iron porphyrin model systems. In the first study to be published,[34] we showed that hydrogen bonding from coordinated imidazole in [Fe(TPP)$(HIm)_2$]Cl (TPP = dianion of *meso*-tetraphenylporphyrin) causes a significant negative shift of the Fe(III)/Fe(II) reduction potential, in agreement with the views given above concerning peroxidases. Negative potential shifts induced by proximal type hydrogen bonding have recently been reported for several other simple bis(imidazole)iron(III) porphyrins.[28,35] Hydrogen bonding *to* an axially coordinated ligand also represents a significant interaction in heme proteins.[36] With the oxygen carriers, the distal histidine can stabilize bound oxygen by this mechanism. Model systems show that hydrogen bonding of the distal type induces positive potential shifts[37] and has a large effect on the axial ligand reactivity.[38-40]

Herein we report electrochemical results showing the influence of proximal type hydrogen bonding on the redox potentials of

(1) Queen Mary College.
(2) Brown University. Recipient, NIH Research Career Development Award, 1983–1988.
(3) Perutz, M. F. *Proc. R. Soc. London, Ser. B* **1980**, *B208*, 135.
(4) Mohr, P.; Scheler, W.; Schumann, H.; Muller, K. *Eur. J. Biochem.* **1967**, *3*, 158.
(5) Morishima, I.; Neya, S.; Yonezawa, T. *Biochem. Biophys. Acta* **1980**, *621*, 218.
(6) Hoq, M. F.; Shepherd, R. E. *Inorg. Chem.* **1984**, *23*, 1851.
(7) Johnson, C. R.; Henderson, W. W.; Shepherd, R. E. *Inorg. Chem.* **1984**, *23*, 2754.
(8) Desbois, A.; Mazza, G.; Stetzkowski, F.; Lutz, M. *Biochim. Biophys. Acta* **1984**, *785*, 161.
(9) Teraoka, J.; Kitagawa, T. *J. Biol. Chem.* **1981**, *256*, 3969.
(10) La Mar, G. N.; de Ropp, J. S. *J. Am. Chem. Soc.* **1982**, *104*, 5203.
(11) La Mar, G. N.; de Ropp, J. S.; Chacko, V. P.; Satterlee, J. D.; Erman, J. E. *Biochim. Biophys. Acta* **1982**, *708*, 317.
(12) Poulos, T. L.; Freer, S. T.; Alden, R. A.; Edwards, S. L.; Skogland, U.; Takio, K.; Eriksson, B.; Xuong, N.; Yonetani, T.; Kraut, J. *J. Biol. Chem.* **1980**, *255*, 575.
(13) Poulos, T. L.; Kraut, J. *J. Biol. Chem.* **1980**, *255*, 8199.
(14) Brautigan, D. L.; Feinberg, B. M.; Margoliash, E.; Peisach, J.; Blumberg, W. E. *J. Biol. Chem.* **1977**, *252*, 574.
(15) Traylor, T. G. *Acc. Chem. Res.* **1981**, *14*, 102.
(16) Valentine, J. S.; Sheridan, R. P.; Allen, L. C.; Kahn, P. C. *Proc. Natl. Acad. Sci. U.S.A.* **1979**, *76*, 1009.
(17) Morrison, M.; Schonbaum, R. *Annu. Rev. Biochem.* **1976**, *45*, 861.
(18) Peisach, J. *Ann. N.Y. Acad. Sci.* **1975**, *244*, 187.
(19) Stein, P.; Mitchell, M.; Spiro, T. G. *J. Am. Chem. Soc.* **1980**, *102*, 7795.
(20) Stanford, M. A.; Swartz, J. C.; Phillips, T. E.; Hoffman, B. M. *J. Am. Chem. Soc.* **1980**, *102*, 4492.
(21) Spiro, T. G. *Isr. J. Chem.* **1981**, *21*, 81.
(22) Chevion, M.; Salhany, J. M.; Peisach, J.; Castillo, C. L.; Blumberg, W. E. *Isr. J. Chem.* **1977**, *15*, 311.
(23) Mincey, T.; Traylor, T. G. *J. Am. Chem. Soc.* **1979**, *101*, 765.
(24) Traylor, T. G.; Mincey, T. C.; Berzinis, A. P. *J. Am. Chem. Soc.* **1981**, *103*, 7084.
(25) Walker, F. A.; Lo, M. W.; Ree, M. T. *J. Am. Chem. Soc.* **1976**, *98*, 5552.
(26) Balch, A. L.; Watkins, J. J.; Doonan, D. J. *Inorg. Chem.* **1979**, *18*, 1228.
(27) Quinn, R.; Nappa, M.; Valentine, J. S. *J. Am. Chem. Soc.* **1982**, *104*, 2588.
(28) Quinn, R.; Strouse, C. E.; Valentine, J. S. *Inorg. Chem.* **1983**, *22*, 3934.
(29) Yoshimura, T.; Ozaki, T. *Arch. Biochem. Biophys.* **1984**, *230*, 466.
(30) Suslick, K. S.; Fox, M. M.; Reinert, T. J. *J. Am. Chem. Soc.* **1984**, *106*, 4522.
(31) Brunori, M.; Saggese, U.; Rotilio, G. C.; Antonini, E.; Wyman, J. *Biochemistry* **1971**, *10*, 1604.
(32) Conroy, C. W.; Tyma, P.; Daum, P. H.; Erman, J. E. *Biochim. Biophys. Acta* **1978**, *537*, 62.
(33) Cassatt, J. C.; Marini, C. P.; Bender, J. *Biochemistry* **1975** *14*, 5470.
(34) Doeff, M. M.; Sweigart, D. A.; O'Brien, P. *Inorg. Chem.* **1983**, *22*, 851.
(35) Quinn, R.; Mercer-Smith, J.; Burstyn, J. N.; Valentine, J. S. *J. Am. Chem. Soc.* **1984**, *106*, 4136.
(36) Mims, M. P.; Porras, A. G.; Olson, J. S.; Noble, R. W.; Peterson, J. A. *J. Biol. Chem.* **1983**, *258*, 14219.
(37) Lexa, D.; Momenteau, M.; Rentien, P.; Rytz, G.; Saveant, J. M.; Xu, F. *J. Am. Chem. Soc.* **1984**, *106*, 4755.
(38) Tondreau, G. A.; Sweigart, D. A. *Inorg. Chem.* **1984**, *23*, 1060 and references therein.
(39) Meng, Q.; Tondreau, G. A.; Edwards, J. O.; Sweigart, D. A., submitted for publication.
(40) Jones, J. G.; Tondreau, G. A.; Edwards, J. O.; Sweigart, D. A., *Inorg. Chem.* **1985**, *24*, 296.

several metalloporphyrins. In particular, the dependence on the solvent, metal, and porphyrin ring substituents are addressed. It is concluded that such hydrogen bonding can substantially affect oxidation state stabilities and, accordingly, should be considered along with other structural features (imidazole ring orientation, Fe–imidazole bond stretch, heme ruffling, etc.) as a mechanism for redox potential modulation in heme proteins.

Experimental Section

Materials. Nitromethane and acetone were dried over molecular sieves and distilled; Me_2SO was vacuum distilled and dried over sieves; dimethylacetamide (DMA), acetonitrile, methylene chloride, and 1,2-dichloroethane (DCE) were distilled from calcium hydride. Imidazole was purified by sublimation, *N*-methylimidazole (*N*-MeIm) was vacuum distilled from KOH, and anhydrous 1,10-phenanthroline (phen) was vacuum dried for 12 h. Hemin chloride (Fe(PPIX)Cl) and Fe(TPP)Cl were purchased and checked for purity by optical spectroscopy. Hemin chloride was esterified to the dimethyl ester (Fe(PPIXDME)Cl) according to a published procedure.[41] [Fe(TPP)]SbF_6,[42] [Fe(TPP)(RIm)$_2$]SbF_6 (R = H, *N*-Me),[35] Ru(TPP)CO,[43] and Ru(TPP)(HIm)CO[44] were synethesized by literature methods. Tetra-*n*-butylammonium tetraphenylborate ((TBA)BPh_4) was made by mixing equal volumes of dilute aqueous solutions of tetra-*n*-butylammonium bromide and sodium tetraphenylborate. The resulting fine precipitate of (TBA)BPh_4 was recrystallized from 1:1 MeOH–H_2O and vacuum dried.

Electrochemistry. Cyclic voltammograms were obtained at 25 °C with a PAR Model 362 scanning potentiostat and a Houston 2000 X-Y recorder or Tektronix Model 5115 storage oscilloscope. A standard three-electrode system was used. The counter electrode was a Pt wire, and the working electrode was a Pt disk. For all solvents except acetone the reference electrode was Ag/AgCl, which was placed in a salt bridge containing 0.1 M tetrabutylammonium perchlorate (TBAP) in the solvent in use. The 0.1 M TBAP salt bridge was also used for experiments in which the bulk solution was 0.05 M in (TBA)BPh_4. With acetone as the solvent the reference electrode consisted of Ag/AgCl in acetone saturated with LiCl; no salt bridge was used in this case. All solutions were deoxygenated with nitrogen presaturated with the appropriate solvent and blanketed with nitrogen during the experiment. With [Fe(TPP)(RIm)$_2$]SbF_6 it was necessary to frequently clean the working electrode to maintain reproducible traces; this was done by dipping the electrode in Me_2SO for ca. 8 min, wiping with a soft tissue, and rinsing with the solvent in use.

Cyclic voltammograms of the Fe(III)/Fe(II) and "Ru(II)/Ru(III)" couples were recorded at scan rates of 20, 50, 100, and 200 mV s^{-1}. At 20 mV s^{-1} the cathodic and anodic peak separations (ΔE_p) were 60–80 mV. These increased slightly with scan rate, e.g., 70–90 mV at 50 mV s^{-1}, with the higher values obtaining in the less polar solvents. This modest deviation of ΔE_p from the reversible value of 60 mV may be due to either uncompensated resistance (*iR* drop) or quasi-reversibility. Most likely *iR* drop is responsible because the ferrocenium/ferrocene couple showed similar behavior, and ΔE_p values for all couples studied were sensitive to electrode placement. Half-wave potentials were calculated as the average of the anodic and cathodic peak potentials and were *independent* of the scan rate. In principle, quasi-reversible behavior should give $E_{1/2}$ values that depend on ΔE_p (hence scan rate) and the deviation of the transfer coefficient (α) from 0.5. However, the dependence in the present work would be barely discernible because the ΔE_p's are not extremely large, and the transfer coefficient was judged to be near 0.5 because of symmetrical anodic and cathodic wave shapes. It follows, therefore, that the measured $E_{1/2}$'s need no correction and that *for the purpose of this study* it is irrelevant whether *iR* drop or quasi-reversibility (or both) is responsible for peak separations greater than 60 mV.

Results and Discussion

Experiments in Acetone. The addition of HIm to an acetone solution of Fe(TPP)Cl causes the Fe(III)/Fe(II) reduction potential to become more positive as [Fe(TPP)(HIm)$_2$]Cl is formed. Figure 2, which gives $E_{1/2}$ values referenced to the ferrocene/ferrocenium couple ($E_{1/2}$(Fc), vide infra), shows that the shift ceases and a plateau region is reached at a HIm concentration of ca. 0.01 M. This occurs because Fe(TPP)Cl is completely converted to [Fe(TPP)(HIm)$_2$]Cl at [HIm] > 0.01 M.[25,38] The interesting aspect of Figure 2 is the subsequent negative potential shift as more HIm is added. The addition of phen to [Fe(TPP)(HIm)$_2$]Cl causes an analogous shift. In both cases proximal type hydrogen bonding (Figure 1) is responsible for the observed behavior.[26,34,35] The decrease in reduction potential of ca. 60 mV[45] is quite substantial and shows, as would be expected, that hydrogen bonding stabilizes the ferric state. Hydrogen bonding of HIm and phen to the coordinated imidazole in [Fe(PPIXDME)(HIm)$_2$]Cl was found to occur in a completely analogous manner, with a cathodic potential shift of ca. 50 mV. Verification of the origin of the cathodic shifts is provided by the observed lack of any potential change with [Fe(TPP)(*N*-MeIm)$_2$]Cl (excess *N*-MeIm = 0.17 M) as phen was added; the value of $E_{1/2} - E_{1/2}$(Fc) remained constant at −602 mV up to the highest phen concentration used (0.43 M). Similarly, it was verified that $E_{1/2}$(Fc) (ca. 670 mV) did not depend on added HIm of phen. (Referencing $E_{1/2}$ to $E_{1/2}$(Fc) is a convenient way to eliminate day to day variations that may occur in the electrodes, especially the reference electrode.)

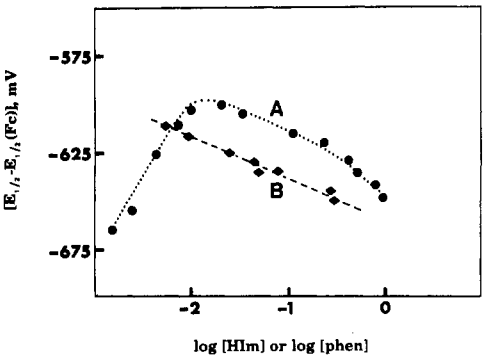

Figure 2. Potential changes of the Fe(III)/Fe(II) couple in acetone with 0.1 M TBAP: (A) 5×10^{-4} M Fe(TPP)Cl plus indicated HIm concentration; (B) 5×10^{-4} M [Fe(TPP)(HIm)$_2$]Cl with [HIm] = 0.02 M and phen concentration as shown.

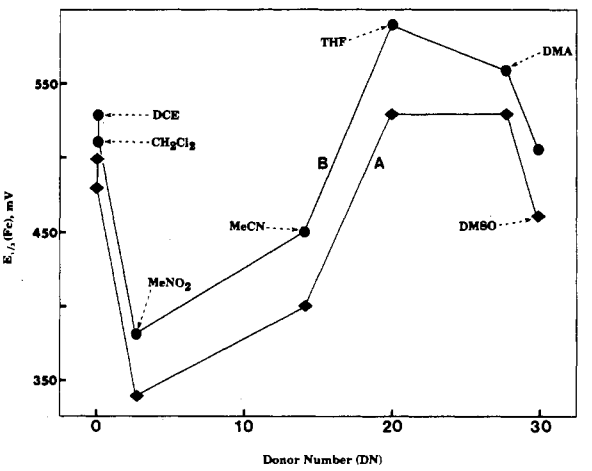

Figure 3. Dependence of $E_{1/2}$ of the ferrocenium/ferrocene couple on solvent donor number: (A) reference electrode SCE (data from ref 48); (B) reference electrode Ag/AgCl. All solutions contain 0.1 M TBAP as supporting electrolyte.

Experiments in Other Solvents. When data in different solvents are compared, there is a good possibility that the liquid-junction potentials will vary among the solvents. Accordingly, it is common practice to reference each potential against a standard couple measured in the same solvent.[46,47] A frequently used reference

(41) Fuhrhop, J.-H.; Smith, K. M. In "Porphyrins and Metalloporphyrins"; Smith, K. M., Ed.; Elsevier: New York, 1975; Chapter 19.
(42) Baldwin, J. E.; Haraldsson, G. G.; Jones, J. G. *Inorg. Chim. Acta* **1981**, *51*, 29.
(43) Tsutsui, M.; Ostfeld, D.; Francis, J. N.; Hoffman, L. M. *J. Coord. Chem.* **1971**, *1*, 115.
(44) Malerich, C. J. *Inorg. Chim. Acta* **1982**, *58*, 123.
(45) In our preliminary communications[34] the shift induced by phen was overestimated as ca. 100 mV due to an erroneous data point at high phen concentration.
(46) Bard, A. J.; faulkner, L. R. "Electrochemical Methods: Fundamentals and Applications"; Wiley: New York, 1980; p 701.
(47) Parker, A. J. *Electrochim. Acta* **1976**, *21*, 671.

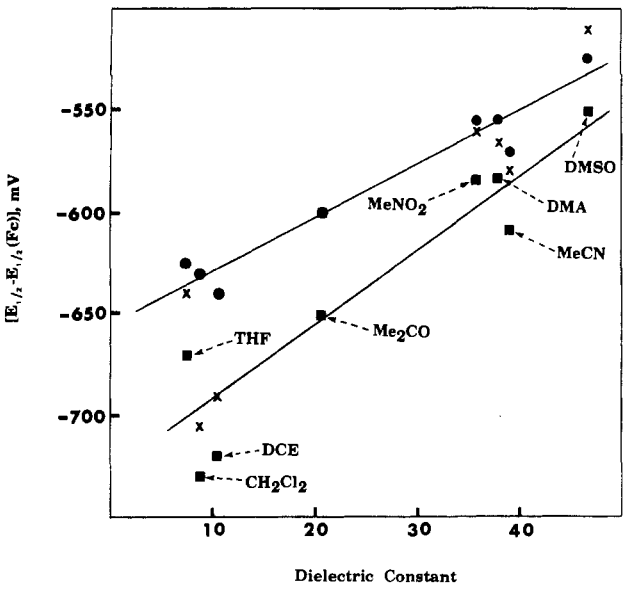

Figure 4. Solvent dependence of $E_{1/2}$ for reduction of [Fe(TPP)(RIm)$_2$]Cl (5×10^{-4} M) relative to $E_{1/2}$(Fc). Supporting electrolyte is 0.1 M TBAP. Key: ●, [Fe(TPP)(*N*-MeIm)$_2$]Cl with 0.16 M *N*-MeIm; ×, [Fe(TPP)(HIm)$_2$]Cl with 0.02 M HIm; ■, [Fe(TPP)(HIm)$_2$]Cl with 1.0 M HIm (0.30 M phen instead of 1.0 M HIm gave almost identical results).

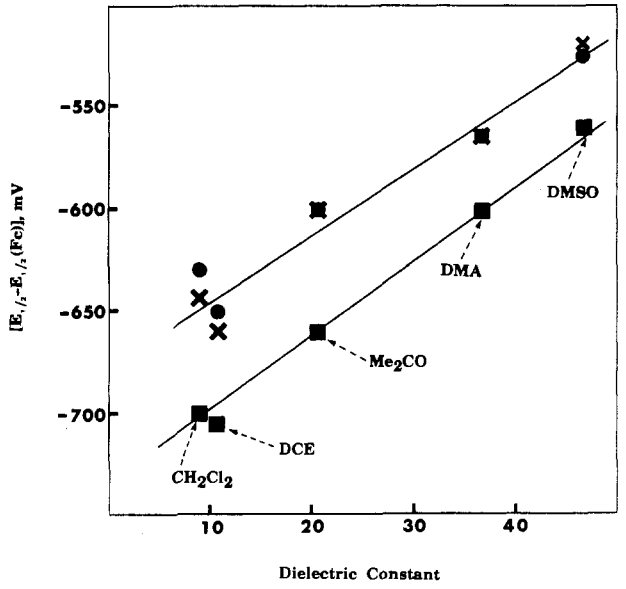

Figure 5. Solvent dependence of $E_{1/2}$ for reduction of [Fe(TPP)(RIm)$_2$]SbF_6 (5×10^{-4} M) relative to $E_{1/2}$(Fc). Supporting electrolyte is 0.05 M (TBA)BPh_4. Key: ●, [Fe(TPP)(*N*-MeIm)$_2$]SbF_6 with 10^{-3} M *N*-MeIm; ×, [Fe(TPP)(HIm)$_2$]SbF_6 with 10^{-3} M HIm; ■, [Fe(TPP)(HIm)$_2$]SbF_6 with 1.0 M HIm.

couple is ferrocenium/ferrocene. The quantity $E_{1/2} - E_{1/2}$(Fc) is then used when the solvent dependence of couple $E_{1/2}$ is to be discussed. This approach has been used in studies of metalloporphyrins.[48-50] The variation with solvent of $E_{1/2}$(Fc) measured with respect to SCE[48] or our aqueous Ag/AgCl reference electrode agrees nicely (Figure 3) but does not correlate with either dielectric constant or solvent donor number (DN).[51] The lack of a correlation to these common solvent parameters may, of course, reflect changing junction potentials.

The solvent dependence of $E_{1/2} - E_{1/2}$(Fc) was determined for [Fe(TPP)(RIm)$_2$]Cl in the presence of phen and excess HIm. Figure 4 shows the correlation to solvent dielectric constant; a qualitatively similar correlation is obtained for a fit to solvent donor number. With [Fe(TPP)(HIm)$_2$]Cl it was necessary in all experiments to have 0.02 M excess HIm present to prevent dissociation to Fe(TPP)Cl. For the same reason, excess *N*-MeIm at 0.16 M was present when [Fe(TPP)(*N*-MeIm)$_2$]Cl was studied. In fact, the *N*-MeIm concentration could be any value greater than 0.16 M without affecting the observed potential. Similarly, Figure 2 shows that the HIm concentration needs to be considerably greater than 0.02 M before the potential is significantly affected by hydrogen bonding.

The formation constant of [Fe(TPP)(RIm)$_2$]SbF_6 is much greater than that for [Fe(TPP)(RIm)$_2$]Cl, and excess RIm is in principle not required with the SbF_6^- salt to prevent RIm dissociation. In practice we found that excess RIm at ca. 10^{-3} M sharpened the anodic wave and improved the reversibility. The cathodic wave was unaffected by excess RIm at 10^{-3} M. The improved reversibility in the presence of small amounts of RIm is probably due to inhibition of RIm dissociation from Fe^{II}(TPP)(RIm)$_2$, which apparently occurs to a small extent in the absence of excess RIm. The important point to note, however, is that the Fe(III)/Fe(II) reduction wave is not influenced by these effects. Figure 5 gives the solvent dependence of $E_{1/2} - E_{1/2}$(Fc) for [Fe(TPP)(RIm)$_2$]SbF_6.

Figures 4 and 5 show that the Fe(III)/Fe(II) reduction becomes easier as the solvent dielectric constant increases. A very similar correlation has been reported for the reduction of Mn(TPP)X (X = N_3^-, ClO_4^-)[49] and Fe(TPP)X (X = N_3^-, F^-, Br^-),[50] and the positive slope in the plot of $E_{1/2} - E_{1/2}$(Fc) vs. dielectric constant in these cases was rationalized as being due to solvation of the charged reduction product. However, this explanation does not apply to the reduction of Fe(TPP)(RIm)$_2^+$ since it predicts a negative slope in Figures 4 and 5. This is so because the reduction product is neutral, and hence increasing solvent polarity should preferentially stabilize the cationic species and lead to a decrease in $E_{1/2}$. The observed positive slope cannot be due to any specific hydrogen-bonding effects with Cl^-, SbF_6^-, or electrolyte anion because $E_{1/2} - E_{1/2}$(Fc) for Fe(TPP)(*N*-MeIm)$_2^+$ follows the same trend seen with the HIm analogue. Ion pairing between the cation and Cl^-, SbF_6^-, or electrolyte anion would be expected to lower the potential and be more pronounced in the less polar solvents and could, therefore, be responsible for the positive slope. However, this seems unlikely because changing the anion X^- in [Fe(TPP)(*N*-MeIm)$_2$]X from SbF_6^- to Cl^- and/or the electrolyte from (TBA)BPh_4 to TBAP causes little or no change in $E_{1/2} - E_{1/2}$(Fc). Were ion pairing important, the change to Cl^- and TBAP should produce a large effect. When interpreting a correlation of $E_{1/2} - E_{1/2}$(Fc) to a solvent parameter, there is an important factor that is usually ignored, namely the solvent dependence of $E_{1/2}$(Fc). It is usually implicitly or explicitly assumed that $E_{1/2}$(Fc) is solvent independent,[52] and indeed this may be a goode assumption when the couple being investigated shows large potential changes with solvent. However, in many cases relatively small variations are involved, and a plot like those in Figures 4 or 5 only shows how $E_{1/2}$ changes relative to any variation in $E_{1/2}$(Fc). Ion-pairing and solvation effects are likely to influence both $E_{1/2}$ and $E_{1/2}$(Fc), and in fact it is very difficult to determine how $E_{1/2}$ depends on solvent without using a variety of reference couples.

Concerning hydrogen-bonding effects, several factors merit discussion. As observed in acetone (vide supra), the $E_{1/2}$ for [Fe(TPP)(*N*-MeIm)$_2$]X in all solvents remained absolutely constant as the concentration of excess *N*-MeIm or of phen was varied, showing that the effects observed with [Fe(TPP)(HIm)$_2$]X are indeed due to hydrogen bonding. Table I lists some data illustrating the potential shifts due to hydrogen bonding to the coordinated HIm. The cathodic shifts upon addition of 1.0 M HIm or 0.30 M phen are similar, suggesting that the hydrogen-bond interactions are comparable. The data in Table I allow some other

(48) Kadish, K. M.; Chang, D. *Inorg. Chem.* **1982**, *21*, 3614.
(49) Kelly, S. L.; Kadish, K. M. *Inorg. Chem.* **1982**, *21*, 3631.
(50) Bottomley, L. A.; Kadish, K. M. *Inorg. Chem.* **1981**, *20*, 1348.
(51) Gutmann, V. "The Donor-Acceptor Approach to Molecular Interactions"; Plenum Press: New York, 1978.
(52) Bauer, D.; Breant, M. *Electroanal. Chem. Interfacial Electrochem.* **1975**, *8*, 282.

Table I. Electrochemical Data for the Reduction of [Fe(TPP)(RIm)$_2$]X at 25 °C

			$E_{1/2} - E_{1/2}$(Fc), mV			
				HIm[c]		
X	solvent	supporting electrolyte[a]	*N*-MeIm[b]			phen[d]
Cl^-	CH_2Cl_2	TBAP	−630	−705	−730	−735
Cl^-	CH_2Cl_2	TBAP[e]	−625	−695	−745	
Cl^-	CH_2Cl_2	(TBA)BPh_4	−620	−640	−690	
SbF_6^-	CH_2Cl_2	(TBA)BPh_4	−630	−645	−700	
Cl^-	acetone	TBAP	−600	−600	−650	−650
SbF_6^-	acetone	(TBA)BPh_4	−600	−600	−660	
Cl^-	DCE	TBAP	−640	−690	−720	−715
SbF_6^-	DCE	(TBA)BPh_4	−650	−660	−705	
Cl^-	DMA	TBAP	−555	−565	−585	−585
SbF_6^-	DMA	(TBA)BPh_4	−565	−565	−600	
Cl^-	Me_2SO	TBAP	−525	−510	−550	
SbF_6^-	Me_2SO	(TBA)BPh_4	−525	−520	−560	
Cl^-	MeCN	TBAP	−570	−580	−610	−615
Cl^-	$MeNO_2$	TBAP	−555	−560	−585	−585
Cl^-	THF	TBAP	−625	−640	−670	−670

[a] TBAP at 0.10 M and (TBA)BPh_4 at 0.05 M, unless stated otherwise. [b] RIm is *N*-MeIm at 0.16 M for X^- = Cl^- and ca. 10^{-3} M for X^- = SbF_6^-. [c] RIm is HIm; the first potential listed is with excess HIm at 0.02 M (X^- = Cl^-) and 10^{-3} M (X^- = SbF_6^-); the second potential is with [HIm] = 1.0 M. [d] Refers to RIm = HIm at 0.02 M, with [phen] = 0.30 M. [e] TBAP = 0.01 M.

interesting conclusions. As stated above, ion pairing by the electrolyte to [Fe(TPP)(*N*-MeIm)$_2$]X is not large since changing from 0.10 M TBAP to 0.05 M (TBA)BPh_4 has little effect on the potential. Similarly, changing X^- from Cl^- to SbF_6^- has little effect. It has been suggested that hydrogen bonding by ClO_4^- to [Fe(TPP)(HIm)$_2$]X in CH_2Cl_2 can be substantial.[35] Table I shows clearly that ClO_4^- associates in this way in the solvents of low dielectric constant and donor number. Thus, in CH_2Cl_2 and DCE the potential of [Fe(TPP)(HIm)$_2$]X is 50–75 mV negative of that for [Fe(TPP)(*N*-MeIm)$_2$]X, whereas in the other more polar solvents the difference is small or zero. As predicted, replacing ClO_4^- by BPh_4^- reduces the difference in CH_2Cl_2 and DCE to a much smaller value (10–20 mV). Similarly, Table I shows that the X^- anions are not hydrogen bonded to coordinated HIm in the more polar solvents (e.g., acetone) and are at least not strongly associated in CH_2Cl_2 and DCE.

The hydrogen-bonding interaction between Fe(TPP)(HIm)$_2^+$ and external HIm and phen can be assessed a number of ways. In CH_2Cl_2 and DCE, the HIm or phen must displace ClO_4^- (and to a lesser degree other anions present) in order to hydrogen bond. Accordingly, the full effect of hydrogen bonding can be assessed by comparing the potential shift between Fe(TPP)(*N*-MeIm)$_2^+$ and Fe(TPP)(HIm)$_2^+$ in the presence of a large excess HIm or phen. This gives an average value of 80 mV for the shift. Taken together, the more polar solvents show an average shift of 40 mV, although in some cases the hydrogen bonding may not be complete under the conditions used, possibly due to competition from the solvent.

Experiments with Ru(TPP)(CO)(HIm). Unlike the case with Fe^{II}(TPP)(RIm)$_2$, the oxidation of Ru(TPP)(CO)(HIm) involves the porphyrin ring and produces a Ru(II) cation radical.[48] In CH_2Cl_2 (0.10 M TBAP) we found that the first oxidation of Ru(TPP)(CO)(HIm) occurs at +805 mV with respect to Ag/AgCl or +290 mV referenced to Fc/Fc$^+$. The addition of phen up to 0.22 M did not affect the potential. This shows that oxidation of Ru(TPP)(CO)(HIm) does not alter the degree of hydrogen bonding to the coordinated imidazole N–H or that no hydrogen bonding occurs in either the reduced or oxidized complex. In either case the reasonable conclusion is reached that redox potential modulation via hydrogen bonding is only important when the redox change is metal centered, thereby directly affecting the metal–imidazole link.

Conclusions. Hydrogen bonding from an external base to coordinated imidazole in an iron porphyrin significantly affects the Fe(III)/Fe(II) redox potential such that the Fe(III) state is stabilized by ca. 60 mV. This potential shift is of sufficient magnitude to be seriously considered as a mechanism of redox potential modulation in heme proteins. The magnitude of the potential shift is moderately solvent dependent but does not seem to depend markedly on the porphyrin ring substituents since Fe(TPP)(HIm)$_2^+$ and Fe(PPIXDME)(HIm)$_2^+$ behave similarly. When the redox change is porphyrin ring centered, as with the oxidation of Ru(TPP)(CO)(HIm), hydrogen-bonding effects seem not to be significant.

Acknowledgment. We are grateful to Dr. J. G. Jones for advice concerning the synthesis of [Fe(TPP)]SbF_6 and to Professor J. O. Edwards for general discussions. This work was supported by grants from the National Institutes of Health (Nos. AM 30145 and AM 01151), NATO (No. 849/83), and the SERC.

Registry No. [Fe(TPP)(MeIm)$_2$]Cl, 41121-76-0; [Fe(TPP)(MeIm)$_2$]SbF_6, 90388-47-9; [Fe(TPP)(HIm)$_2$]Cl, 25442-52-8; [Fe(TPP)(HIm)$_2$]SbF_6, 80939-25-9; phen, 66-71-7; TBAP, 1923-70-2; (TBA)BPh_4, 15522-59-5; [Fe(PPIXDMF)(HIm)$_2$]Cl, 20467-68-9; Ru(TPP)(CO)(HIm), 32242-24-3; HIm, 288-32-4; *N*-MeIm, 616-47-7.